

The influence of the transition zone water filter on convective circulation in the mantle

Garrett M. Leahy and David Bercovici

Department of Geology and Geophysics, Yale University, New Haven, Connecticut, USA

Received 5 August 2004; revised 24 October 2004; accepted 8 November 2004; published 8 December 2004.

[1] The “transition zone water filter” model of mantle convection attempts to reconcile geochemical evidence for isolated mantle reservoirs with geophysical evidence for whole mantle circulation by decoupling incompatible elements from bulk mantle circulation via a melt layer above the 410 km discontinuity. This would result in a stratified heating distribution similar to layered convection models, but would permit bulk mass and heat transfer across mantle interfaces. Here we test the basic effect of the water filter mechanism on mantle flow, in particular to see whether it induces layered convection and/or strong upwelling plumes above strongly heated layers. We investigate the influence of ten likely heating distributions on the planform of convection. Excepting an extreme case where all heating occurs in the transition zone, convection is not significantly influenced by the heating distribution. For Earth-like internal heating, the flow is dominated by downwellings which extend across the entire model mantle, as in uniformly internally heated layers.

INDEX TERMS: 8121 Tectonophysics: Dynamics, convection currents and mantle plumes; 8124 Tectonophysics: Earth’s interior—composition and state (1212); 8130 Tectonophysics: Heat generation and transport; 8199 Tectonophysics: General or miscellaneous. **Citation:** Leahy, G. M., and D. Bercovici (2004), The influence of the transition zone water filter on convective circulation in the mantle, *Geophys. Res. Lett.*, *31*, L23605, doi:10.1029/2004GL021206.

1. Introduction

[2] A persistent problem in the study of mantle dynamics is the reconciliation of geochemical evidence for isolated mantle source regions for mid-ocean ridge basalts and ocean island basalts [e.g., *van Keken et al.*, 2002] with geophysical evidence for whole mantle convection (e.g., subducting slabs and upwelling plumes seismically inferred to extend into the lower mantle [e.g., *van der Hilst et al.*, 1997; *Montelli et al.*, 2004]). Various models have been proposed [e.g., *van Keken and Ballentine*, 1998; *Coltice and Ricard*, 1999; *Kellogg et al.*, 1999] to explain these observations through some form of chemical stratification or layering. However, there is no evidence for impermeable boundaries in the mantle [*Masters et al.*, 2000]. Additionally, models that invoke layering require most heat producing elements in the mantle to be isolated in the enriched lower layer, which necessitates strong thermal boundary layers near the interface between layers leading to large upwellings [*Tackley*, 2002], which are not consistent with estimates of

plume flux [e.g., *Davies*, 1988; *Sleep*, 1990]. A new model proposed by *Bercovici and Karato* [2003] circumvents these inconsistencies by decoupling incompatible (heat producing) elements from bulk mantle circulation via the “transition zone water filter” mechanism.

[3] In the water filter theory, subducting slabs force up a broad background of passively upwelling ambient mantle that is hydrated as it passes through the possibly water-rich transition zone. As the upwelling passes out of the transition zone, the phase change to low water-solubility olivine forces dehydration melting. This melt (which is presumed heavy) extracts incompatible elements and accumulates above the 410 km discontinuity. Water and trace elements are recycled back into the lower mantle via slab entrainment, where the colder temperatures near slabs allow the melt to crystallize in the wadsleyite phase, and be dragged into the lower mantle. This mechanism keeps incompatibles including heat producing elements sequestered beneath the 410 km discontinuity similar to layered mantle models. The resulting layered heat distribution could significantly affect convective circulation by basally heating the upper (above 410 km) mantle, as would occur in layered mantle models. However, *Bercovici and Karato* [2003] stipulate that since mass and heat transport are not impeded by the filter mechanism, there should be little effect on the overall circulation.

[4] Here we test a basic aspect of the water filter mechanism by investigating the effect of layered internal heating distributions on convective circulation, e.g., whether transfer of slabs to the lower mantle is prohibited, or excessively large plumes are initiated in the upper mantle. We investigate the effect of ten likely heating distributions on the onset of convection and on finite-amplitude convection.

2. Governing Equations

[5] For the sake of simplicity and focusing on the essential problem of inhomogeneous heat source distributions, we consider 2D convection (in the x - z plane) in an Boussinesq, constant viscosity fluid with infinite Prandtl number. The equations of mass, momentum, and energy conservation lead to dimensionless governing equations for temperature anomalies (relative to conductive state) θ and velocity stream function ψ (such that velocity $\mathbf{v} = \nabla \times \psi \hat{\mathbf{y}}$)

$$\frac{\partial \theta}{\partial t} - \hat{\mathbf{y}} \cdot (\nabla \psi \times \nabla \theta) + \frac{\partial \psi}{\partial x} \frac{d\theta_c}{dz} = \nabla^2 \theta, \quad (1)$$

$$\nabla^4 \psi + Ra \frac{\partial \theta}{\partial x} = 0, \quad (2)$$

where the static conductive temperature profile θ_c satisfies

$$\frac{d^2\theta_c}{dz^2} + \frac{Ra_H}{Ra}\Gamma(z) = 0, \quad (3)$$

and $\Gamma(z)$ is the depth dependent heat source distribution (see section 3). The Rayleigh numbers for basal heating and internal heating are

$$Ra = \frac{\rho_0 \alpha g \Delta T d^3}{\mu \kappa} \quad \text{and} \quad Ra_H = \frac{\rho_0 \alpha g H d^5}{\mu \kappa k}, \quad (4)$$

respectively.

[6] In equations (1)–(4), μ is viscosity, ρ_0 is reference density, α is thermal expansivity, g is acceleration due to gravity, t is time, κ is thermal diffusivity, k is thermal conductivity, H is averaged volumetric heat production. We consider only the case of isothermal, impermeable, free-slip top and bottom boundaries and use periodic vertical boundary conditions. The boundary conditions are then $\psi = \frac{\partial^2 \psi}{\partial z^2} = \theta = \theta_c - (1 - z) = 0$; at $z = 0, 1$. There are no mechanical boundary conditions at the interior interfaces (e.g., the 410 or 660 km discontinuities) as they are considered permeable.

3. Heating Distributions

[7] In this study, we consider ten possible distributions of heating elements and study their effect on convection. The distribution function $\Gamma(z)$ is defined as a sum of Heaviside functions $\mathcal{H}(z - z_i)$ with coefficient vector $\mathbf{a} = (a_1, a_2, a_3)$ determining step height in the lower mantle ($0 < z < .77$), transition zone ($.77 \leq z \leq .86$), and the upper mantle ($.86 < z < 1$):

$$\Gamma(z) = a_1[1 - \mathcal{H}(z - .77)] + a_2[\mathcal{H}(z - .77) - \mathcal{H}(z - .86)] + a_3\mathcal{H}(z - .86). \quad (5)$$

\mathbf{a} is constrained by $\int_0^1 \Gamma(z) dz = 1$.

[8] In addition to the whole-mantle uniform heating control (case 1), there are two end member heat distributions that are predicted by the water filter model, assuming all heat producing elements are removed from the upwelling mantle at the 410. The first of these assumes that when incompatibles are returned to the lower mantle via slab entrainment, they are efficiently mixed into the lower mantle. This would result in an even distribution of radiogenic elements in the mantle below 410 km (case 2). The other end member assumes that as the entrained (water saturated and incompatible rich) material passes downward through the 660 km discontinuity and changes phase to the lower water solubility magnesium perovskite phase, excess water is exsolved, which extracts incompatible elements and buoyantly returns to the transition zone. At peak efficiency, the water exsolution mechanism could trap all heat producing elements in the transition zone (case 3). In reality, we expect this to mechanism to work inefficiently, leading to partial exsolution of heat producing elements (case 4, a mix between cases 2 and 3), possibly due to one of the following reasons. First, chemical disequilibrium during the dehydration process could permit some incompatibles to continue

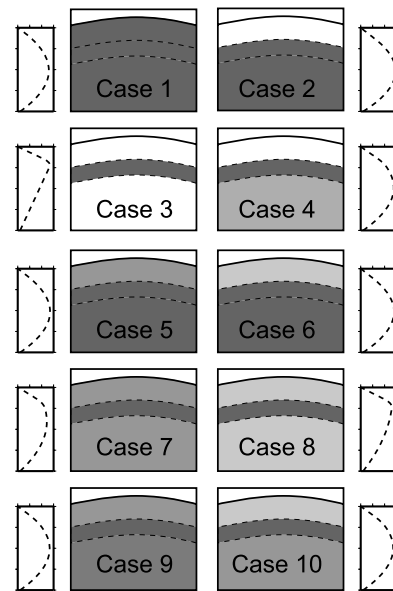


Figure 1. Heating distributions for the ten cases described in section 3, with shading indicating relative intensities. The conductive temperature profile associated with each heating distribution is plotted next to each case.

into the lower mantle, resulting in a hybrid distribution. Another possible mechanism would be if there existed downwelling regions containing relatively dry enriched oceanic crust. This would limit exsolution of water and therefore more incompatibles would return to the lower mantle. In both cases we consider a scenario where heating in the transition zone is about 2.5 times the heating in the lower mantle, in order to simulate the effect of incompatibles partially exsolved at the 660 km discontinuity. This number is poorly constrained, but for the purpose of this study we estimate it based on the premise that all incompatibles filtered from the upper (above 410 km) mantle return to the transition zone, where they join a background concentration evenly distributed below 410 km. We also consider the effects of the addition of background secular cooling to the above distributions [Weinstein and Olson, 1990]. This term represents the volume-integrated heat loss of the system. Though in reality this cooling term is likely temporally variable, for simplicity we treat it as a constant part of the internal heat term. Depending on the original bulk silicate earth composition preferred, 1/3 to 2/3 of heat from the mantle can be attributed to secular cooling [e.g., Schubert et al., 2001; Rocholl and Jochum, 1993]. We model the end member cases by adding secular cooling in a ratio to radiogenic heat of either 2:1 (cases 5, 7, and 9) or 1:2 (cases 6, 8, and 10).

[9] For the Earth, we expect the distribution of heating elements to be some combination of the following cases (see also Figure 1):

[10] Case 1: Whole-mantle uniform heating (no water filter); $\mathbf{a} = (1, 1, 1)$.

[11] Case 2: Uniform heating below the 410, corresponding to efficient recycling of incompatibles; $\mathbf{a} = (1.16, 1.16, 0)$.

[12] Case 3: All heating in the transition zone corresponding to all heating elements being extracted from

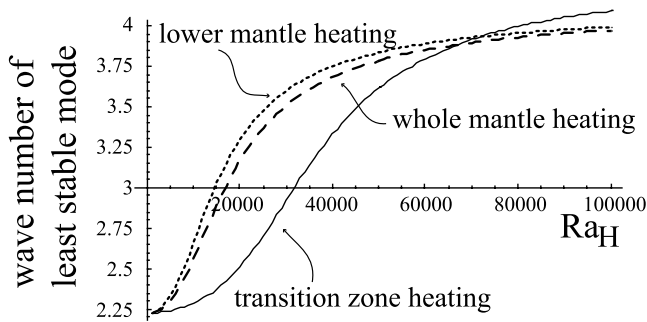


Figure 2. Marginal stability of an internally heated layer: Least stable mode versus Ra_H for whole mantle heating (case 1, dashed), lower mantle heating (case 2, dotted), and transition zone heating (case 3, solid).

downgoing slabs due to dehydration after slabs pass through the 660 km discontinuity; $\mathbf{a} = (0, 11.11, 0)$.

[13] Case 4: Partial extraction of incompatibles from slabs into the transition zone, and remaining incompatibles distributed into the lower mantle (mix between cases 2 and 3); $\mathbf{a} = (1, 2.56, 0)$.

[14] Case 5: Secular cooling in the whole mantle with uniform heat from incompatibles below the 410, in a ratio of 2:1; $\mathbf{a} = (1.05, 1.05, .67)$.

[15] Case 6: Same as case 5 but with secular cooling half the magnitude of radiogenic heat production (a ratio of 1:2); $\mathbf{a} = (1.11, 1.11, .33)$.

[16] Case 7: Secular cooling in the whole mantle with heat from incompatibles locked up in the transition zone, in a ratio of 2:1; $\mathbf{a} = (.67, 4.37, .67)$.

[17] Case 8: Same as case 7 but with secular cooling half the magnitude of radiogenic heat production (a ratio of 1:2); $\mathbf{a} = (.33, 7.74, .33)$.

[18] Case 9: Secular cooling in the whole mantle with partial extraction of incompatibles into the transition zone, the rest are evenly distributed in the lower mantle (a mix between cases 5 and 7, with secular cooling and radiogenic heat in a ratio of 2:1); $\mathbf{a} = (1, 1.52, .67)$.

[19] Case 10: Same as case 9 but with secular cooling half the magnitude of radiogenic heat production (a ratio of 1:2); $\mathbf{a} = (1, 1.70, .33)$.

4. Marginal Stability

[20] We first consider the marginal stability of the system to examine the effect of the water filter mechanism on the basic planform of convection [Sparrow *et al.*, 1964]. This analysis yields the horizontal wavelength of the dominant convective cell at the onset of convection (least stable mode). Combining linearized versions of equations (1) and (2) yields

$$\nabla^6 \psi = -Ra \frac{\partial^2 \psi}{\partial x^2} \frac{d\theta_c}{dz}. \quad (6)$$

[21] In addition, we can infer that all even derivatives of ψ with respect to z vanish at the boundaries which allows us to write

$$\psi(x, z) = \sum_{n=0}^{\infty} \psi_n e^{ikx} \sin(n\pi z), \quad (7)$$

where $k \in \mathcal{R}$ is the horizontal wave number and n is the vertical mode. Following the method of Chandrasekhar [1961], we combine equations (7) and (6), and then Fourier transform in z . This yields a matrix equation of the form $\sum A_{mn} \psi_n = 0$, where the elements of the matrix \underline{A} are defined as follows:

$$A_{mn} = \left((n\pi)^2 + k^2 \right) \frac{3\delta_{mn}}{2} + Ra k^2 \int_0^1 \frac{\partial \theta_c}{\partial z} \sin(m\pi z) \sin(n\pi z) dz. \quad (8)$$

[22] This matrix must be subject to the condition $\det \underline{A} = 0$ which provides a characteristic equation for the critical Ra that can then be solved, depending on the number of desired vertical modes n , horizontal wave number k , and conductive profile $\theta_c(z)$.

[23] In applying this technique to our study, we consider the extreme end member distributions, and compare them to the whole mantle heating case. Therefore we examine the effect of Ra_H on the least stable mode for uniform (step-function) heating in the lower mantle (case 2) and the transition zone box-car (case 3). Figure 2 shows that for sufficiently high Ra_H , the wave number of the least stable mode doubles, but this behavior is not significantly influenced by the heating distribution.

5. Nonlinear Convection

[24] We use a pseudo-spectral code [benchmarked against linear solutions of section 4 and Travis *et al.*, 1990, with $Ra_H = 0$] to solve equations (1) and (2). We present 10 numerical convection experiments with the heating distributions listed in section 3, with Earth-like Rayleigh numbers $Ra = 10^6$ and $Ra_H = 10^8$ [Schubert *et al.*, 2001]. Our simulations show that except for extreme cases where all heating elements are trapped in the transition zone (case 3), the water filter mechanism would have little effect on the convective planform. All of the other distributions we consider do not differ remarkably from a uniform distribution (case 1).

[25] In most of the cases, we find that the convective style is similar to the purely internally heated case (case 1), where heat transport is dominated by slabs. In our experiment, we find that downwellings penetrate easily into the heated region, reaching almost to the very bottom. A slightly colder (and therefore stable) region forms at the bottom of the model due to penetrative cooling, and appears to reach a steady thickness.

[26] In case 3 (Figure 3, case 3), however, we find a markedly different style of convection. The highly heated region at the top of the box results in an almost gravitationally stable lower region. Heat transport in the region above the bottom of the model transition zone is dominated by downwellings, which appear to penetrate easily into the heated region, but lose their signature at the bottom of the transition zone. In this case, however, the wavelength of the downwellings tends to be shorter than in the other cases. In Figure 3, case 3, we include stream lines to demonstrate that though the thermal anomaly fades as downwellings pass out of the transition zone, there is mass transfer across the boundary and the whole model mantle is participating in

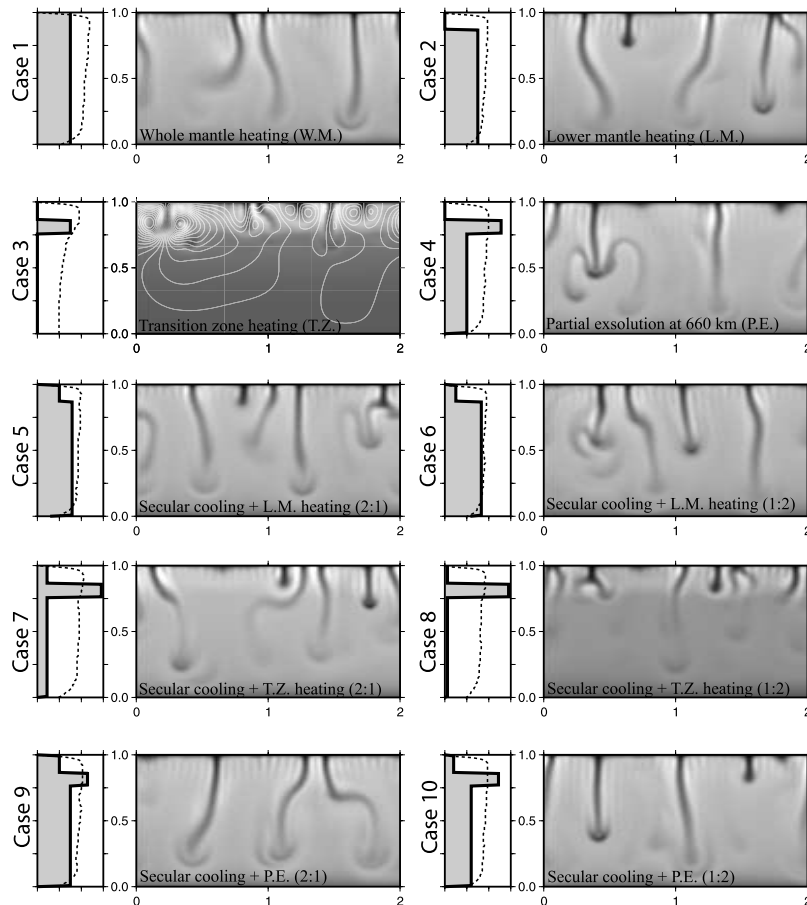


Figure 3. Convection experiments: Temperature field and heating distributions for the 10 cases considered in this study. For each case, the left frame gives the heating distribution $\Gamma(z)$ (shaded area) and the horizontally averaged heating temperature (dashed line). The right frame for each case is the total temperature field, where white represents hot regions and black represents cold regions. In case 3, stream lines have been added to demonstrate the whole region participates in the convective cycle even though the lower layer appears stable.

the convective cycle. The influence of the near-stable region on the size of the convective region likely dictates a smaller wavelength, but this was not apparent from the marginal stability problem.

6. Discussion and Conclusion

[27] Our results show that for the case where heating elements are sequestered below the 410 km discontinuity, the style of convection is dominated by downwellings that easily penetrate into the lower model mantle. This style is similar to that predicted by current seismic models. The persistence of slabs in the lower mantle is likely underestimated by our model, as we allow the slabs to be heated from the inside at the same rate as the lower mantle. In practice, this is likely not the case, and slabs may persist to greater depths. We confirm the stipulation of *Bercovici and Karato* [2003] that permitting mass transfer at mantle interfaces does not result in heating the upper mantle from below, and therefore there are no mid-mantle boundary layers leading to unrealistically large plumes.

[28] The boxcar experiment's (case 3) failure to resemble large scale seismic observations reinforces the belief that any heated layer should extend to the bottom of the mantle. However, cases 7 and 8 demonstrate that some degree of

secular cooling can serve to mitigate the effects of intense heating in the transition zone. More sophisticated physical models would have an effect on these results. On the one hand, the addition of phase transitions would serve to enhance layered structure. However, temperature dependent and other nonlinear rheologies would enhance whole-mantle flow, as cold, stiff slabs would penetrate more easily into the lower regions of the model.

[29] However, the simple assumptions of our model indicate that a mechanism to redistribute incompatible heating elements from the transition zone to the lower mantle would be preferred based on our view of mantle flow. Possible mechanisms for this scenario include disequilibrium effects during dehydration, or limited water exsolution due to the subduction of dry oceanic crust. Both of these possibilities would be a consequence of the low diffusivities of heat producing elements versus the fast percolation of water back into the transition zone [*Bercovici and Karato*, 2003]. We therefore conclude hybrid cases 9 and 10 would be more plausible heat distributions for a mantle with an active water filter.

[30] **Acknowledgments.** We would like to thank Jeroen van Hunen, Shun-ichiro Karato, Jun Korenaga, and an anonymous reviewer for their comments on this manuscript. This work was supported under a

National Science Foundation Graduate Research Fellowship and NSF grant EAR-0330745.

References

- Bercovici, D., and S. Karato (2003), Whole mantle convection and the transition-zone water filter, *Nature*, *425*, 39–44.
- Chandrasekhar, S. (1961), *Hydrodynamic and Hydromagnetic Stability*, Oxford Univ. Press, New York.
- Coltice, N., and Y. Ricard (1999), Geochemical observations and one layer mantle convection, *Earth Planet. Sci. Lett.*, *174*, 125–137.
- Davies, G. (1988), Ocean bathymetry and mantle convection: 1. Large-scale flow and hotspots, *J. Geophys. Res.*, *93*, 10,467–10,480.
- Kellogg, L., B. Hager, and R. van der Hilst (1999), Compositional stratification in the deep mantle, *Science*, *283*, 1881–1884.
- Masters, G., G. Laske, H. Bolton, and A. Dziewonski (2000), The relative behavior of shear velocity, bulk sound speed, and compressional velocity in the mantle: Implications for chemical and thermal structure, in *Earth's Deep Interior: Mineral Physics and Tomography From the Atomic to the Global Scale*, *Geophys. Monogr. Ser.*, vol. 117, edited by S. Karato et al., pp. 63–87, AGU, Washington, D. C.
- Montelli, R., G. Nolet, F. A. Dahlen, G. Masters, E. R. Engdahl, and S. Hung (2004), Finite-frequency tomography reveals a variety of plumes in the mantle, *Science*, *303*, 338–343.
- Rocholl, A., and K. Jochum (1993), Th, U, and other trace elements in carbonaceous chondrites—Implications for the terrestrial and solar system Th/U ratios, *Earth Planet. Sci. Lett.*, *117*, 265–278.
- Schubert, G., D. Turcotte, and P. Olson (2001), *Mantle Convection in the Earth and Planets*, Cambridge Univ. Press, New York.
- Sleep, N. (1990), Hotspots and mantle plumes: Some phenomenology, *J. Geophys. Res.*, *95*, 6715–6736.
- Sparrow, E., R. Goldstein, and V. Jonsson (1964), Thermal instability in a horizontal fluid layer: Effect of boundary conditions and non-linear temperature profile, *J. Fluid Mech.*, *18*, 513–528.
- Tackley, P. J. (2002), Strong heterogeneity caused by deep mantle layering, *Geochem. Geophys. Geosyst.*, *3*(4), 1024, doi:10.1029/2001GC000167.
- Travis, B. J., C. Anderson, J. Baumgardner, C. W. Gable, B. H. Hager, R. J. O'Connell, P. Olson, A. Raefsky, and G. Schubert (1990), A benchmark comparison of numerical methods for infinite Prandtl number thermal convection in two-dimensional Cartesian geometry, *Geophys. Astrophys. Fluid Dyn.*, *55*, 137–160.
- van der Hilst, R. D., S. Widiyantoro, and E. R. Engdahl (1997), Evidence for deep mantle circulation from global tomography, *Nature*, *386*, 578–584.
- van Keken, P. E., and C. J. Ballentine (1998), Whole-mantle versus layered mantle convection and the role of a high-viscosity lower mantle in terrestrial volatile evolution, *Earth Planet. Sci. Lett.*, *156*, 19–32.
- van Keken, P., E. Hauri, and C. Ballentine (2002), Mantle mixing: The generation, preservation, and destruction of chemical heterogeneity, *Annu. Rev. Earth Planet. Sci.*, *30*, 493–525.
- Weinstein, S., and P. Olson (1990), Planforms in thermal convection with internal heat sources at large Rayleigh and Prandtl numbers, *Geophys. Res. Lett.*, *17*, 239–242.

D. Bercovici and G. M. Leahy, Department of Geology and Geophysics, Yale University, P.O. Box 208109, New Haven, CT 06520-8109, USA. (garrett.leahy@yale.edu)